

CHAPTER 14

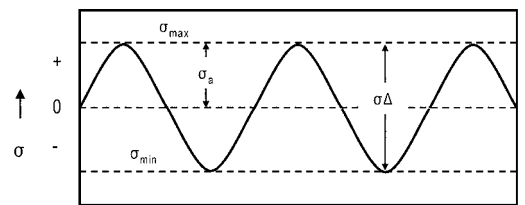
Fatigue

FATIGUE FAILURES OCCUR due to the application of fluctuating stresses that are much lower than the stress required to cause failure during a single application of stress. It has been estimated that fatigue contributes to approximately 90% of all mechanical service failures. Fatigue is a problem that can affect any part or component that moves. Automobiles on roads, aircraft wings and fuselages, ships at sea, nuclear reactors, jet engines, and land-based turbines are all subject to fatigue failures. Fatigue was initially recognized as a problem in the early 1800s when investigators in Europe observed that bridge and railroad components were cracking when subjected to repeated loading. As the century progressed and the use of metals expanded with the increasing use of machines, more and more failures of components subjected to repeated loads were recorded. Today, structural fatigue has assumed an even greater importance as a result of the ever-increasing use of high-strength materials and the desire for higher performance from these materials.

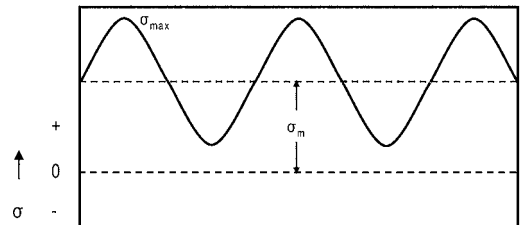
14.1 Stress Cycles

There are three basic factors necessary to cause fatigue: (1) a maximum tensile stress of sufficiently high value, (2) a large enough variation or fluctuation in the applied stress, and (3) a sufficiently large number of cycles of the applied stress. There are many types of fluctuating stresses. Several of the more common types encountered are shown in Fig. 14.1. A fully reversed stress cycle, shown in the top graph of Fig. 14.1, where the maximum and minimum stresses are equal, is commonly used in testing. This is the type of stress produced, for example, by the R.R. Moore rotating-beam fatigue machine shown in Fig. 14.2, which is similar to what a shaft may encounter during service. Since this was the original type of machine used to generate fatigue data, quite a bit

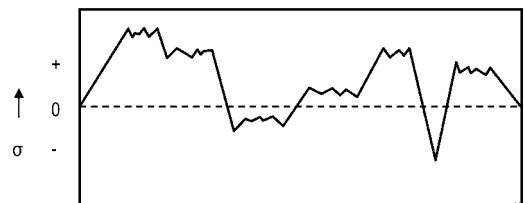
of the data in the literature is for fully reversed bending with no mean stress applied on top of it. Another common stress cycle is the repeated stress cycle, in which there is a mean stress (σ_m) applied on top of the maximum and minimum



Fully Reversed Loading



Tension-Tension with Applied Stress



Random or Spectrum Loading

Cyclic Stress Range: $\sigma_{\Delta} = \sigma_{\max} - \sigma_{\min}$
Cyclic Stress Amplitude: $\sigma_a = \frac{\sigma_{\max} - \sigma_{\min}}{2}$
Mean Stress: $\sigma_m = \frac{\sigma_{\max} + \sigma_{\min}}{2}$
Stress Ratio: $R = \frac{\sigma_{\min}}{\sigma_{\max}}$

Fig. 14.1 Typical loading cycles

244 / Elements of Metallurgy and Engineering Alloys

stresses. The middle graph in Fig. 14.1 shows the condition where both stresses (cyclic and applied) are tensile (greater than zero), but it is also possible to test with both stresses in compression. In addition, the maximum and minimum stresses in the cycle do not necessarily have to be equal in value. The last type of loading cycle is the random or irregular stress cycle, in which the part is subjected to random loads during service, as shown in the bottom graph of Fig. 14.1. Although a majority of the fatigue data in the literature is for fully reversed bending, there are also axial test machines (Fig. 14.3) that are capable of tension and compression loading in both the high- and low-cycle fatigue ranges. These modern test frames are closed-loop servohydraulically controlled and can be programmed with almost any desired fatigue spectrum.

A fluctuating stress is made up of two components: a mean or steady stress, σ_m , and an alternating or variable stress, σ_a . The stress range, σ_r , is the difference between the maximum and minimum stress in a cycle:

$$\sigma_r = \sigma_{\max} - \sigma_{\min} \quad (\text{Eq 14.1})$$

The alternating stress is one-half the stress range:

$$\sigma_a = \frac{\sigma_r}{2} = \frac{\sigma_{\max} - \sigma_{\min}}{2} \quad (\text{Eq 14.2})$$

The mean stress is the algebraic average of the maximum and minimum stress in the cycle:

$$\sigma_m = \frac{\sigma_{\max} + \sigma_{\min}}{2} \quad (\text{Eq 14.3})$$

Two ratios frequently used in presenting fatigue data are:

$$\text{Stress ratio} \quad R = \frac{\sigma_{\min}}{\sigma_{\max}} \quad (\text{Eq 14.4})$$

$$\text{Amplitude ratio} \quad A = \frac{\sigma_a}{\sigma_m} = \frac{1-R}{1+R} \quad (\text{Eq 14.5})$$

14.2 High-Cycle Fatigue

High-cycle fatigue involves a large number of cycles ($N > 10^5$ cycles) and an elastically applied stress. High-cycle fatigue tests are usually carried out for 10^7 cycles and sometimes 5×10^8 cycles for nonferrous metals. Although the applied stress is low enough to be elastic, plastic deformation can take place at the crack tip. High-cycle fatigue data are usually presented as a plot of stress, S , versus the number of cycles to failure, N . A log scale is used for the number of cycles. The value of stress, S , can be the maximum stress, σ_{\max} , the minimum stress, σ_{\min} , or the stress amplitude, σ_a . The $S-N$ relationship is usually determined for a specified value of the mean stress, σ_m , or one of the two ratios, R or A .

The fatigue life is the number of cycles to failure at a specified stress level, while the fatigue strength (also referred to as the endurance limit) is the stress below which failure does not occur. As the applied stress level is decreased, the number of cycles to failure increases. Normally, the fatigue strength increases as the static tensile strength increases. For example,

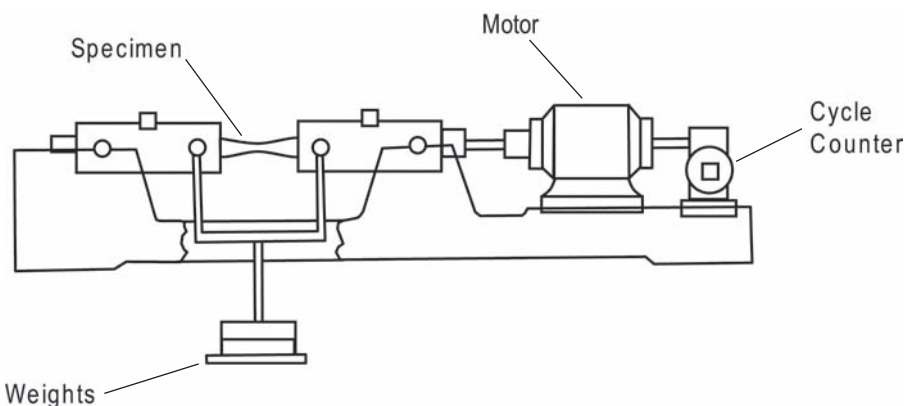


Fig. 14.2 Schematic of R.R. Moore reversed-bending fatigue machine. Source: Ref 1

high-strength steels heat treated to over 1400 MPa (200 ksi) yield strengths have much higher fatigue strengths than aluminum alloys with 480 MPa (70 ksi) yield strengths. A comparison of the $S-N$ curves for steel and aluminum is shown in Fig. 14.4. Note that steel not only has a higher fatigue strength than aluminum, but it also has an endurance limit. Below a certain stress level, the steel alloy will never fail due to cyclic loading alone. On the other hand, aluminum does not have a true endurance limit. It will always fail if tested to a sufficient number of cycles. Therefore, the fatigue strength of aluminum is usually reported as the stress level it can survive at a large total number of cycles, usually 5×10^8 cycles. It should be noted that there is a considerable amount of scatter in fatigue test results. It is therefore important to test a sufficient number of specimens to obtain statistically meaningful results.

For a large number of steels, there is a direct correlation between tensile strength and fatigue strength; higher-tensile-strength steels have higher endurance limits. The endurance limit is normally in the range of 0.35 to 0.60 of the tensile strength. This relationship holds up to a hardness of approximately 40 HRC (~1200 MPa, or 180 ksi tensile strength), and

then the scatter becomes too great to be reliable (Fig. 14.5). This does not necessarily mean it is wise to use as high a strength steel as possible to maximize fatigue life because, as the tensile strength increases, the fracture toughness decreases and the environmental sensitivity increases. The endurance limit of high-strength steels is extremely sensitive to surface condition, residual-stress state, and the presence of inclusions that act as stress concentrations.

Fatigue cracking can occur quite early in the service life of the component by the formation of a small crack, generally at some point on the external surface. The crack then propagates slowly through the material in a direction roughly perpendicular to the main tensile axis (Fig. 14.6). Ultimately, the cross-sectional area of the member is reduced to the point that it can no longer carry the load, and the member fails in tension. The fracture surface of a fatigued high-strength part is shown in Fig. 14.7. The portion of the fracture surface due to fatigue crack growth and the portion finally cracked due to overload are clearly evident.

As previously mentioned, much of the fatigue data in the literature has been determined for completely reversed bending with $\sigma_m = 0$. However, the effects of mean stress are important,

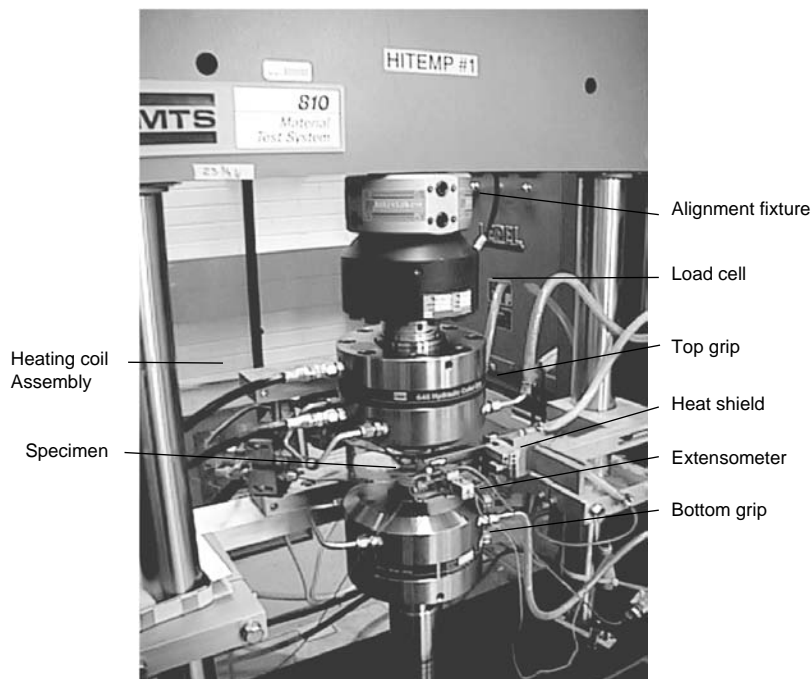


Fig. 14.3 Modern fatigue test frame

246 / Elements of Metallurgy and Engineering Alloys

and an increase in mean stress will always cause a reduction in the fatigue life (Fig. 14.8). A number of mathematical models have been developed that allow the effects of mean stress on stress amplitude to be predicted from fully reversed-bending data. Goodman developed a linear model, while Gerber used a parabolic model (Fig. 14.9). Test data for ductile metals

usually fall closer to the Gerber parabolic curve; however, because of the scatter in fatigue data and the fact that notched data fall closer to the Goodman line, the more conservative Goodman relationship is often used in practice. If the component design is based on yield rather than ultimate strength, as most are, then the even more conservative Soderberg relationship can be used. Mathematically, the three relationships can be expressed by:

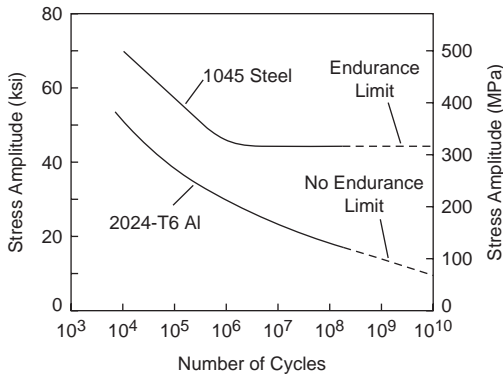


Fig. 14.4 Comparison of steel and aluminum fatigue behavior. Source: Ref 2

$$\sigma_a = \sigma_e \left[1 - \left(\frac{\sigma_m}{\sigma_u} \right)^x \right] \quad (\text{Eq 14.6})$$

where $x = 1$ for the Goodman line, $x = 2$ for the Gerber curve, $\sigma_u = \sigma_y$ for the Soderberg curve, and σ_e is the fatigue limit for completely reversed bending.

14.3 Low-Cycle Fatigue

During cyclic loading within the elastic regime, stress and strain are directly related through the elastic modulus. However, for cyclic

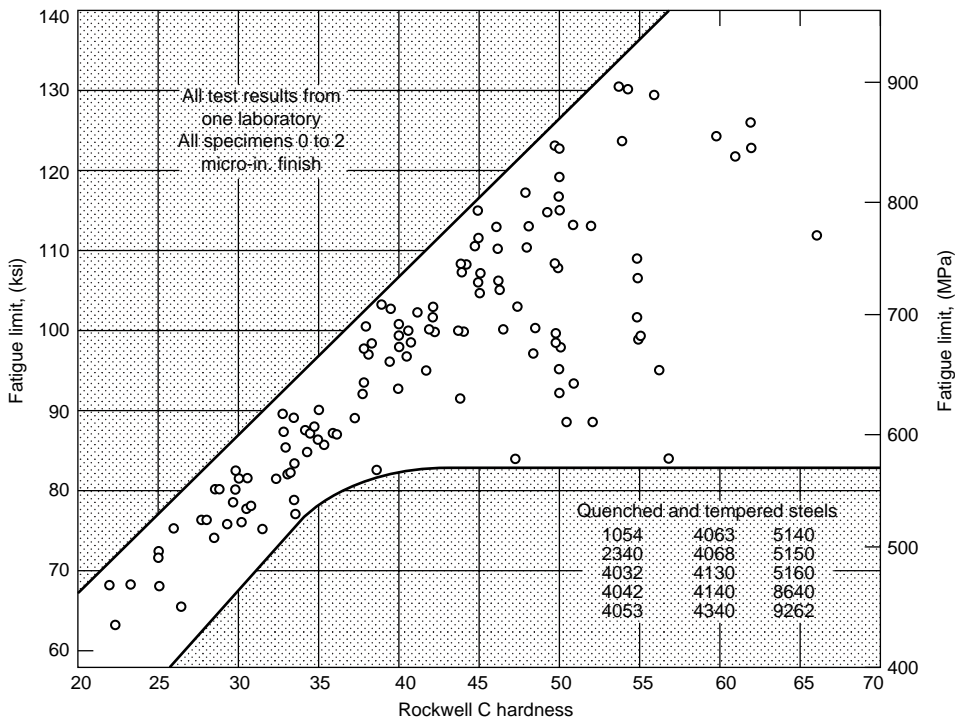


Fig. 14.5 Endurance limit versus hardness for steels. Source: Ref 3

loading that produces plastic strains, the responses are more complex and form a hysteresis loop (Fig. 14.10). From point *O* up to point *A*, the component is in tension. On unloading, the strain response of the specimen follows the curve from *A* to *D*. At *D*, the component is under no stress. As the component is subjected to compressive stress, the strain response follows the curve from *D* to *B*. Releasing the compressive stress from *B* and reapplying tensile stress, the component stress-strain condition returns to point *A* along the curve defined by *B*, *C*, and *A*. Points *A* and *B* represent the cyclic stress and strain limits. The total strain,

$\Delta\varepsilon$, consists of both elastic and plastic components:

$$\Delta\varepsilon = \Delta\varepsilon_e + \Delta\varepsilon_p \quad (\text{Eq 14.7})$$

where $\Delta\varepsilon_e$ is the elastic strain and $\Delta\varepsilon_e = \Delta\sigma/E$, and $\Delta\varepsilon_p$ is the plastic strain and $\Delta\varepsilon_p$ is the width of the loop at its center, that is, the distance *CD* in Fig. 14.10. The area of the hysteresis loop is equal to the work done or the energy loss per cycle.

In cyclic strain-controlled fatigue, the strain amplitude is held constant during cycling. Since plastic deformation is not completely

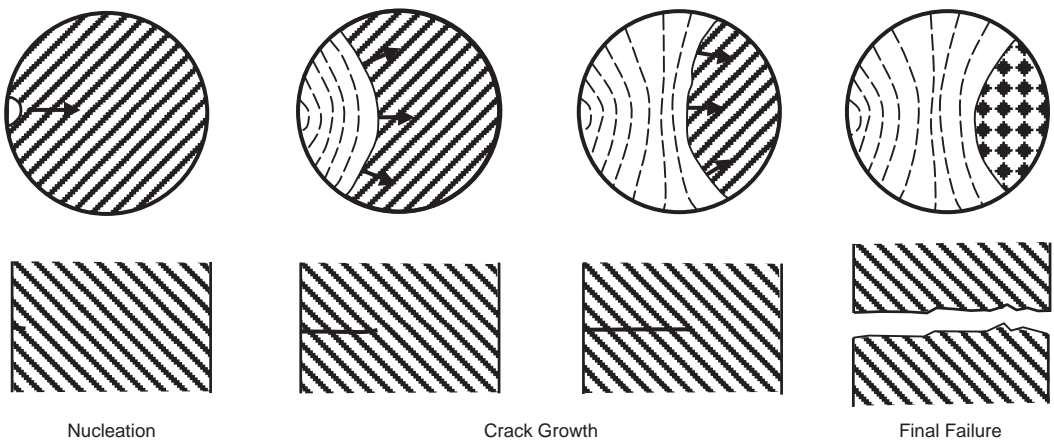


Fig. 14.6 Typical propagation of a fatigue crack. Source: Ref 4

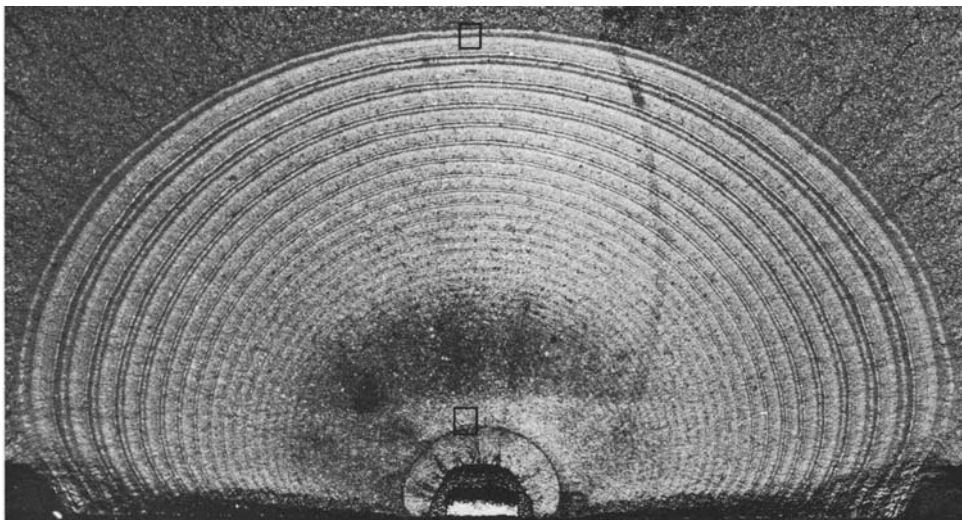


Fig. 14.7 Fatigue crack growth in a high-strength steel part

248 / Elements of Metallurgy and Engineering Alloys

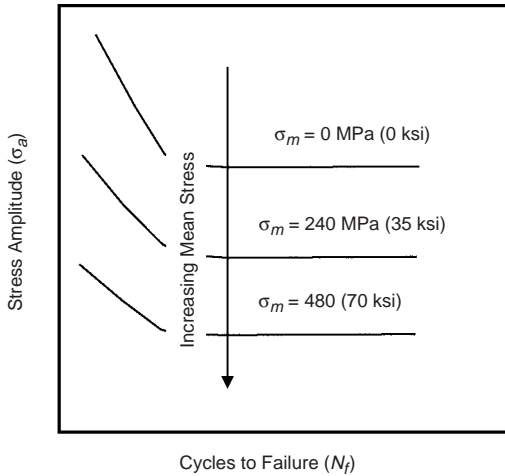
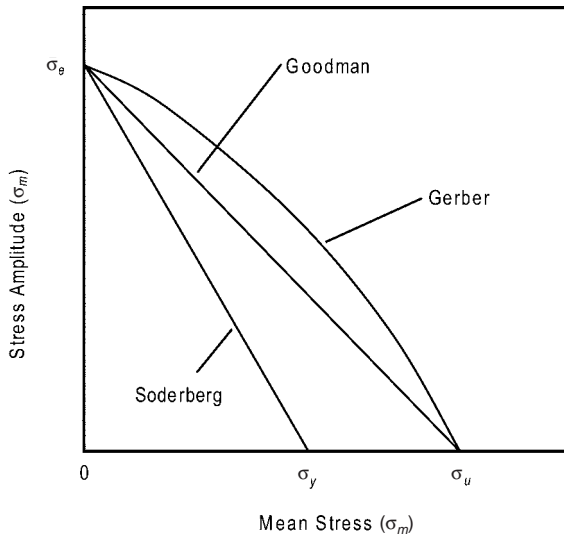


Fig. 14.8 Effect of mean stress on fatigue life

reversible, the stress-strain response during cycling can change, largely depending on the initial condition of the metal. The metal can either undergo cyclic strain hardening, cyclic strain softening, or remain stable. Cyclic strain hardening and softening are illustrated schematically in Fig. 14.11. In both cases, the hysteresis loops change with successive cycles. Cyclic hardening leads to increasing peak strain with increasing cycles, while cyclic softening results in decreasing strain levels with increasing cycles. In general, strong metals tend to cyclically soften, and low-strength metals tend to cyclically harden. However, the hysteresis loop tends to stabilize after a few hundred cycles, when the material attains a stable condition for the imposed strain level.



$$\begin{aligned} \text{Goodman} \quad \sigma_a &= \sigma_e \left[1 - \left(\frac{\sigma_m}{\sigma_u} \right) \right] & \text{Soderberg} \quad \sigma_a &= \sigma_e \left[1 - \left(\frac{\sigma_m}{\sigma_y} \right) \right] \\ \text{Gerber} \quad \sigma_a &= \sigma_e \left[1 - \left(\frac{\sigma_m}{\sigma_u} \right)^2 \right] \end{aligned}$$

where

- σ_e = Fatigue strength for N cycles under zero mean stress
- σ_a = Fatigue strength for N cycles under mean stress of σ_m
- σ_u = Ultimate tensile strength
- σ_y = Yield strength

Fig. 14.9 Comparison of Goodman, Gerber, and Soderberg models for relating mean stress to stress amplitude

Typically, metals harden if $\sigma_u/\sigma_y \geq 1.4$ and soften if $\sigma_u/\sigma_y \leq 1.2$.

The reason for hardening or softening is related to the dislocation microstructure of the metal. When the metal is highly work hardened and the dislocation density is high, cyclic strain allows the rearrangement of dislocations into more stable networks, thereby reducing the stress at which plastic deformation occurs. Conversely, when the initial dislocation density is low, the cyclic strain increases the dislocation density, increasing the amount of elastic strain and stress on the material.

Low-cycle fatigue test data are often presented as a plot of the plastic strain range, $\Delta\epsilon_p$, versus cycles to failure, N . When plotted on log-log coordinates, a straight line is obtained that is described by the Coffin-Manson relation:

$$\frac{\Delta\epsilon_p}{2} = \epsilon'_f (2N)^c \quad (\text{Eq 14.8})$$

where $\Delta\epsilon_p/2$ is the plastic strain amplitude, and ϵ'_f is the fatigue ductility coefficient defined by the strain intercept at $2N = 1$. For many metals,

ϵ'_f is approximately equal to the true fracture strain, ϵ_f . $2N$ is the number of strain reversals to failure, where one cycle is two reversals, and c is the fatigue ductility exponent, which usually varies between -0.5 and -0.7 . A smaller value of c results in longer fatigue lives.

The Basquin equation, which describes the high-cycle, low-strain regime where the nominal strains are elastic, is:

$$\sigma_a = \frac{\Delta\epsilon_e}{2} E = \sigma'_f (2N)^b \quad (\text{Eq 14.9})$$

where σ_a is the alternating stress amplitude, $\Delta\epsilon_e/2$ is the elastic strain amplitude, E is the modulus of elasticity, and σ'_f is the fatigue strength coefficient, defined as the stress intercept at $2N = 1$. σ'_f is approximately equal to the true fracture stress, σ_f . $2N$ is the number of load reversals to failure, and b is the fatigue strength exponent, which varies for most metals between -0.05 and -0.12 . A smaller b results in a longer fatigue life.

Combining Basquin's equation and the Coffin-Manson equation gives an equation

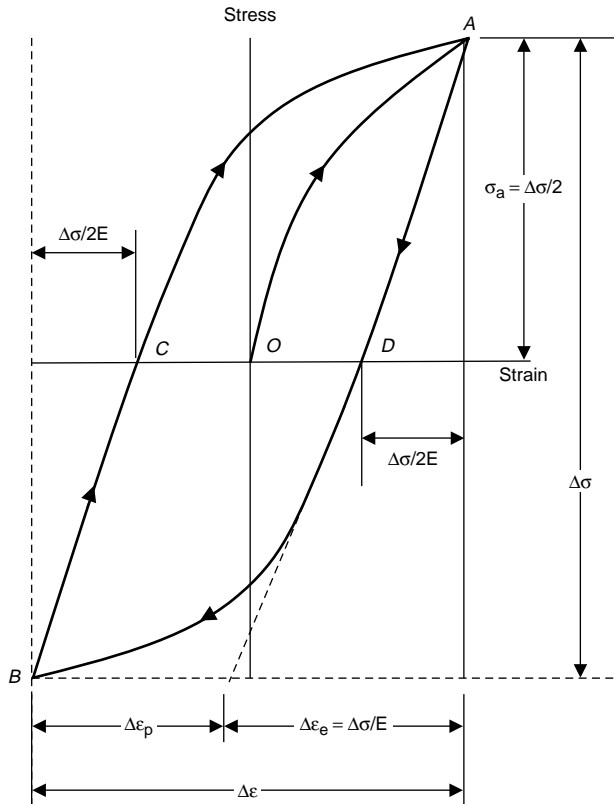


Fig. 14.10 Stress-strain hysteresis loop for cyclic loading

250 / Elements of Metallurgy and Engineering Alloys

that can be used to estimate the entire range of fatigue lives:

$$\frac{\Delta \epsilon}{2} = \frac{\sigma'_f}{E} (2N)^b + \epsilon'_f (2N)^c \quad (\text{Eq 14.11})$$

$$\frac{\Delta \epsilon}{2} = \frac{\Delta \epsilon_e}{2} + \frac{\Delta \epsilon_p}{2} \quad (\text{Eq 14.10})$$

The fatigue strain-life curve tends toward the plastic curve at large strain amplitudes and

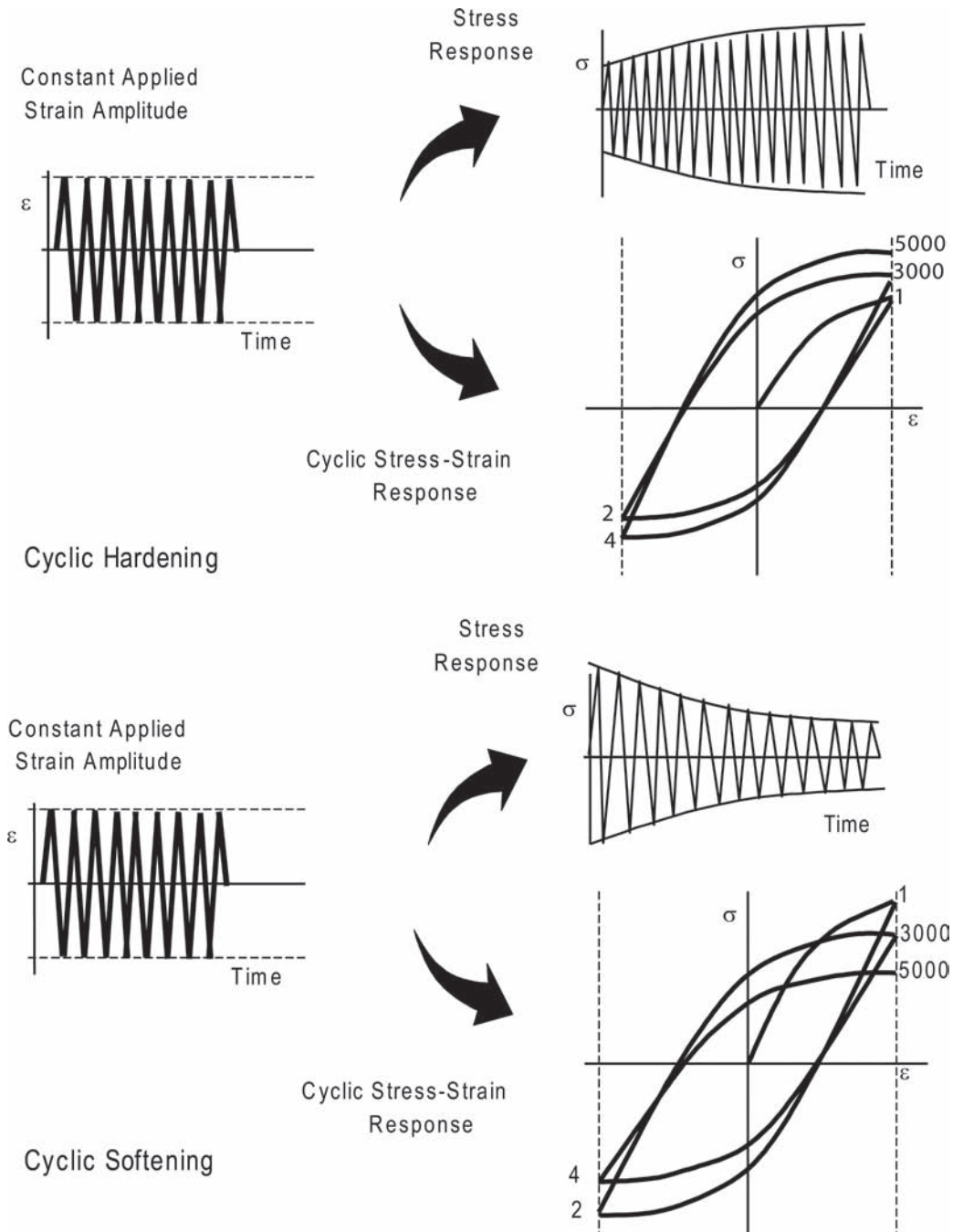


Fig. 14.11 Cyclic hardening and cyclic softening

14.5 Fatigue Crack Nucleation and Growth

Fatigue cracks almost always initiate at free surfaces, usually external surfaces but also internal surfaces if the metal contains defects such as voids and cracked second-phase particles. Common external surface defects include geometric notches and surface roughness.

Fatigue crack nucleation and growth occurs in the following stages.

Stage I. Crack initiation usually starts at a notch or other surface discontinuity. Even in the absence of a surface defect, crack initiation will eventually occur due to the formation of persistent slip bands (PSBs), so called because traces of the bands persist even when the surface damage is polished away. Slip bands are a result of the systematic buildup of fine slip movements on the order of only 1 nm. However, the plastic strain within the PSB can be as much as 100 times greater than that in the surrounding material. The back-and-forth movement of the slip bands leads to the formation of intrusions and extrusions at the surface, eventually leading to the formation of a crack (Fig. 14.14). The initial crack propagates parallel to the slip bands. The crack propagation rate during stage I is very low, on the order of 1 nm per cycle, and produces a practically featureless fracture surface. The crack initially follows the slip bands at approximately 45° to the principal stress direction. When the crack length becomes sufficient for the stress field at the tip to become dominant, the overall crack plane changes and becomes perpendicular to the principal stress, and the crack enters stage II.

Stage II crack growth occurs when the stage I crack changes direction and propagates in a

direction normal to the applied stress. Crack growth proceeds by a continual process of crack sharpening followed by blunting, as shown in the Fig. 14.15 illustration. Crack propagation during crack growth often produces a pattern of fatigue striations (Fig. 14.16), with each striation representing one cycle of fatigue. Although striations are indicative of fatigue, fatigue failures can occur without the formation of striations. Striations are microstructural details that are best examined with a scanning electron microscope and are not visible to the naked eye. Frequently, visible examination of a fatigued surface will reveal a series of concentric markings on the surface, referred to as beach marks (Fig. 14.6). These are present as a result of stress changes during fatigue, for example, the starting and stopping of a rotating shaft. Each of the beach marks can contain thousands or even tens of thousands of fatigue cycles.

Stage III. Ultimate failure occurs when the fatigue crack becomes long enough that the remaining cross section can no longer support the applied load.

14.6 Fatigue Crack Propagation

Linear elastic fracture mechanics assumes that all structures contain flaws. Cracks grow from an initial size, a_0 , to a critical size, a_c , corresponding to failure as a function of the number of load cycles (Fig. 14.17). The crack growth rate, da/dn , can be determined from the slope of the curve. Initially, the crack growth rate is slow but increases with increasing crack length. Of course, the crack growth rate is also higher for higher applied stresses. If one can characterize the crack growth, it is then possible to estimate

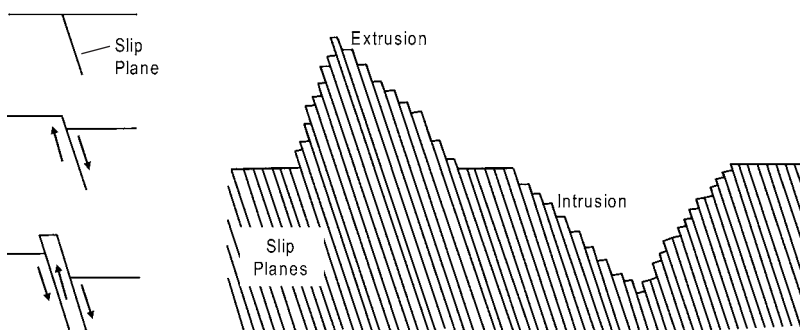


Fig. 14.14 Development of extrusions and intrusions during fatigue. Source: Ref 4

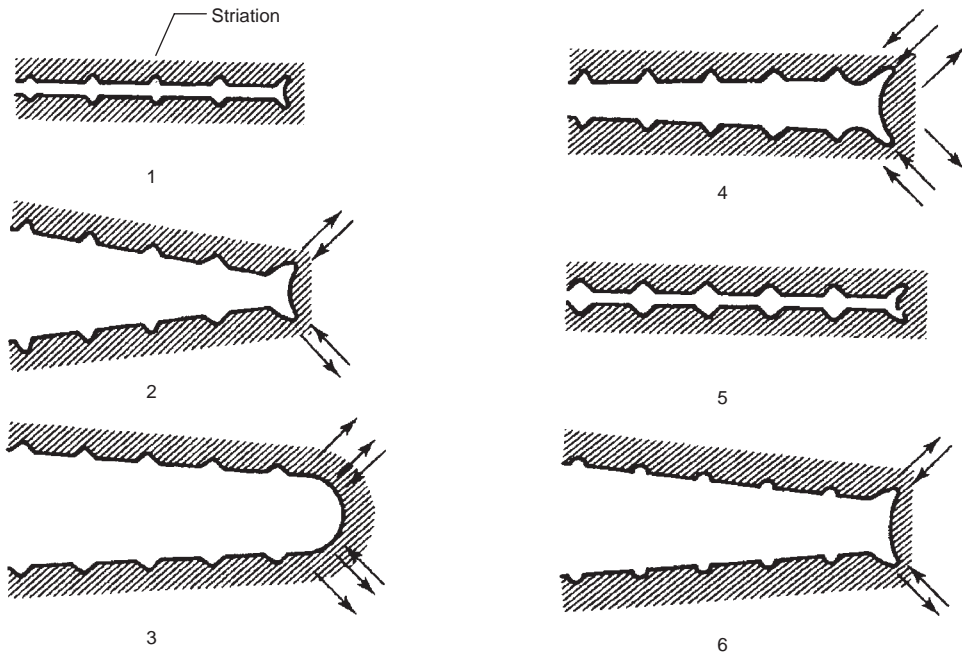


Fig. 14.15 Fatigue crack propagation. Source: Ref 6

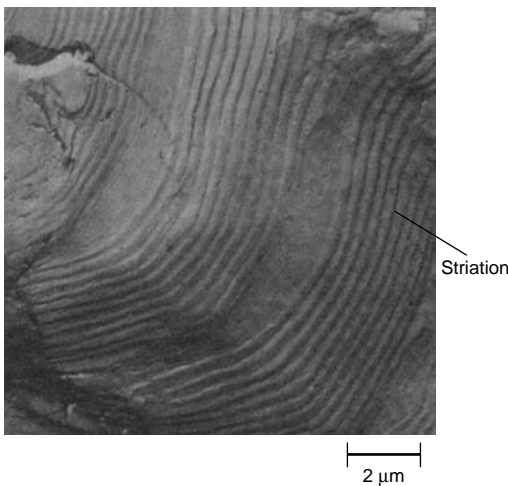


Fig. 14.16 SEM image showing fatigue striations

the service life or inspection intervals required under specific loading conditions and service environment. In the fracture mechanics approach to fatigue crack growth, the crack growth rate, or the amount of crack extension per loading cycle, is correlated with the stress-intensity parameter, K . This approach makes it possible to estimate the useful safe lifetime and to establish

inspection intervals. An idealized da/dn versus ΔK curve is shown in Fig. 14.18. In region I, ΔK_{th} is the fatigue crack growth threshold, which is at the lower end of the ΔK range, where crack growth rates approach zero. In region II, the crack growth rate is stable and essentially linear and can be modeled by power law equations, such as the Paris equation:

$$da/dn = C(\Delta K)^m \quad (\text{Eq 14.13})$$

where: a is the flaw or crack size in inches; n is the number of cycles; C and m are constant parameters and are related to material variables, environment, temperature, and fatigue stress conditions; and $\Delta K = \Delta K_{max} - \Delta K_{min}$ is the stress-intensity parameter range. The constants C and m are material parameters that must be determined experimentally. Typically, m is in the range of 2 to 4 for metals and 4 to 100 for ceramics and polymers.

During stage II growth in the linear crack growth region, the Paris law can be used to determine the number of cycles to failure. ΔK can be expressed in terms of $\Delta\sigma$:

$$\begin{aligned} \Delta K &= \Delta K_{max} - \Delta K_{min} = Y\sigma_{max} \\ &\times \sqrt{\pi a} - Y\sigma_{min} \sqrt{\pi a} = Y\Delta\sigma \sqrt{\pi a} \end{aligned} \quad (\text{Eq 14.14})$$

254 / Elements of Metallurgy and Engineering Alloys

where Y depends on the specific specimen geometry. Thus, the Paris law becomes:

$$\frac{da}{dn} = C(Y\Delta\sigma\sqrt{\pi a})^m \quad (\text{Eq 14.15})$$

One of the goals of fatigue analysis is to be able to predict the fatigue life of structures. The fatigue life, n , can be solved for by rearranging Eq 14.13:

$$dn = \frac{da}{C(\Delta K)^m} \quad (\text{Eq 14.16})$$

which may then be integrated to give:

$$n_f = \int_0^{n_f} dn = \int_{a_0}^{a_c} \frac{da}{C(\Delta K)^m} \quad (\text{Eq 14.17})$$

Substitution of the expression for ΔK (Eq 14.14) gives:

$$n_f = \int_{a_0}^{a_c} \frac{da}{C(Y\Delta\sigma\sqrt{\pi a})^m} = \frac{1}{C\pi^{m/2}(\Delta\sigma)^m} \int_{a_0}^{a_c} \frac{da}{Y^m a^{m/2}} \quad (\text{Eq 14.18})$$

It is assumed that $\Delta\sigma$ (or $\sigma_{\max} - \sigma_{\min}$) is constant and that Y depends on the crack length and therefore cannot be removed from within the integral. For cases where Y depends on crack length, these integrations will generally be performed using numerical techniques. During stage II crack growth, some metals are sensitive to the load ratio, R , as shown in Fig. 14.19 for

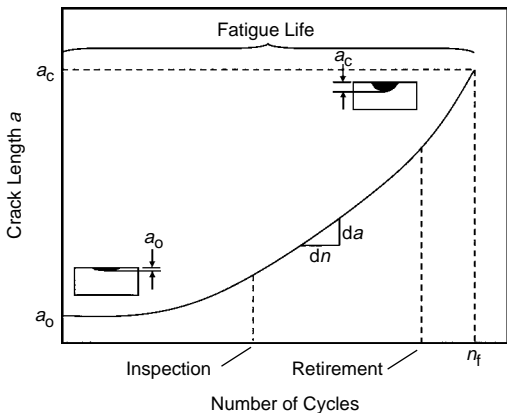


Fig. 14.17 Crack length as a function of cycles. Source: Ref 5

7075-T651 aluminum plate. Since the Paris equation does not account for the load ratio, there are other expressions that do account for the sensitivity of crack growth rate to the load ratio. One of the most utilized is the one developed by Foreman and his associates:

$$\frac{da}{dn} = \frac{C(\Delta K)^m}{(1-R)K_c - \Delta K} \quad (\text{Eq 14.19})$$

In these expressions, it is necessary to determine the initial crack length, a_0 , and the final or critical crack length, a_c . Crack lengths can be detected using a number of nondestructive testing techniques. If no cracks are detected, it must be assumed that a crack exists below the resolution of the detection system being used. A subcritical crack will eventually grow to a length at which the metal immediately fails, that is:

$$K_{\max} \rightarrow K_c \quad (\text{Eq 14.20})$$

or

$$Y\sigma_{\max}\sqrt{\pi a_f} \rightarrow K_c \quad (\text{Eq 14.21})$$

Solving for a_c gives:

$$a_c = \frac{K_c^2}{\pi Y^2 \sigma_{\max}^2} \quad (\text{Eq 14.22})$$

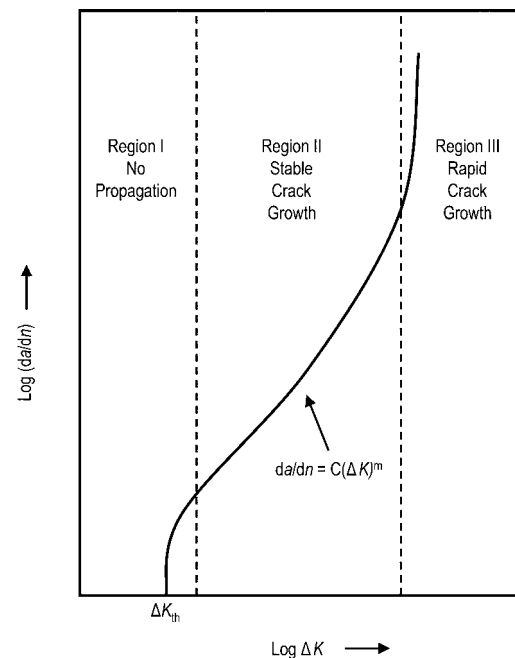


Fig. 14.18 Crack propagation curve for fatigue loading

Note that even if a component contains a detectable crack, it can remain in service, provided that it is periodically inspected. This philosophy forms the basis for what is known as the damage-tolerance design approach.

Finally, in region III, the crack growth rate accelerates, since the fracture toughness of the material is approached, and there is a local tensile overload failure.

14.7 Crack Closure

During fatigue cycling, the crack growth rate can slow due to crack closure. For example, if the structure is subjected to a series of high-tensile overloads that are followed by loads at lower tensile stress levels, the crack may temporarily stop propagating, leading to a decrease in the crack growth rate, da/dN , and consequently have

a longer fatigue life than would normally be expected. Crack closure mechanisms effectively reduce the ΔK during fatigue cycling, thus retarding the crack growth. Since ΔK is equal to $K_{max} - K_{min}$ and the actual ΔK is reduced because crack closure is hindered, ΔK is effectively smaller, and crack growth rate is then reduced.

Four mechanisms that can cause crack closure are shown in Fig. 14.20. Plasticity-induced closure results from compressive residual stresses developing in the plastic wake. Roughness-induced closure is due to crack meandering, in which the crack deviates from mode I displacements and is subject to mode II shear displacements. These displacements cause a mismatch between the upper and lower crack faces, which results in contact between the crack faces during cycling. Oxide debris-induced closure results from corrosion products becoming wedged in the crack interface. Finally, fluid

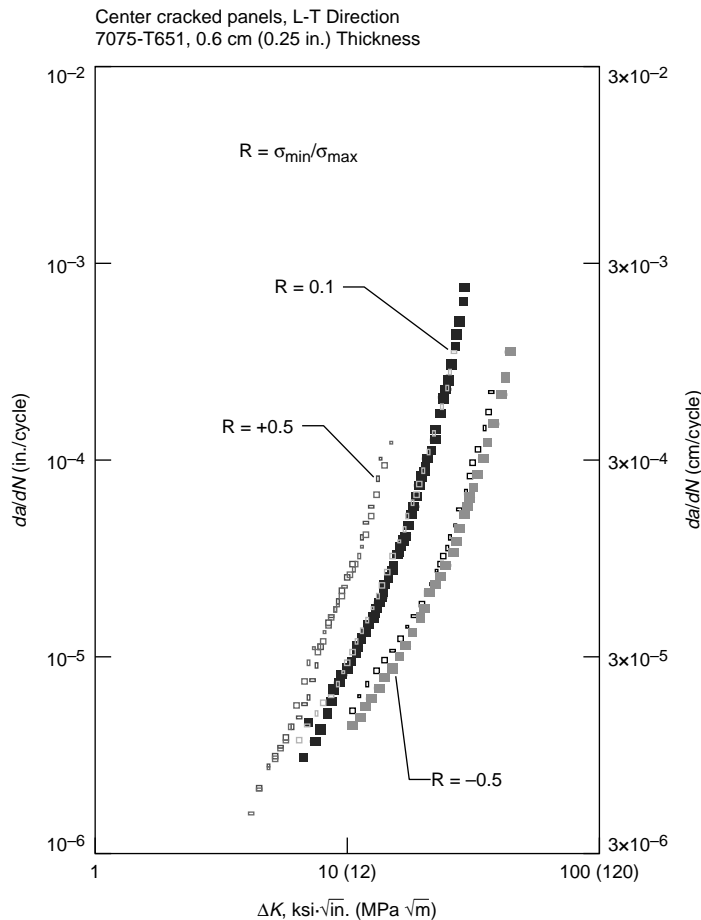


Fig. 14.19 Stress ratio effects on an aluminum alloy

256 / Elements of Metallurgy and Engineering Alloys

pressure can act as a wedge, preventing total crack closure.

14.8 Geometrical Stress Concentrations

In most structures, fatigue cracking usually initiates at a stress concentration. The stress concentration may be inherent in the design, such as a fillet, hole, thread, or other geometrical feature, or the stress concentration can result from a manufacturing process, such as a rough surface finish or residual tensile stresses introduced by heat treatment.

The effect of geometrical stress concentrations on fatigue is often studied by testing notched specimens. When a notch is present in a specimen under uniaxial loading, three effects are present: (1) there is an increase or concentration of stress at the root of the notch, (2) there is a stress gradient from the notch toward the center of the specimen, and (3) a triaxial state of stress exists. The dramatic reduction in

fatigue life of normalized 4340 steel sheet containing different types of stress concentrations is shown in Fig. 14.21.

The effect of notches on fatigue strength is determined by comparing the *S-N* curves of notched and unnotched specimens. The data for the notched specimens are usually plotted in terms of nominal stress based on the net cross section of the specimen. The effect of the notch in decreasing the fatigue strength is reported as the fatigue strength reduction factor, or the fatigue notch factor, K_f :

$$K_f = \frac{\text{Fatigue limit unnotched}}{\text{Fatigue limit notched}} \quad (\text{Eq 14.23})$$

For metals that do not have a definite fatigue limit, the fatigue notch factor is based on the fatigue strength at a specified number of cycles. Values of the fatigue notch factor vary with the severity of the notch, the type of notch, the material, the type of loading, and the applied stress level.

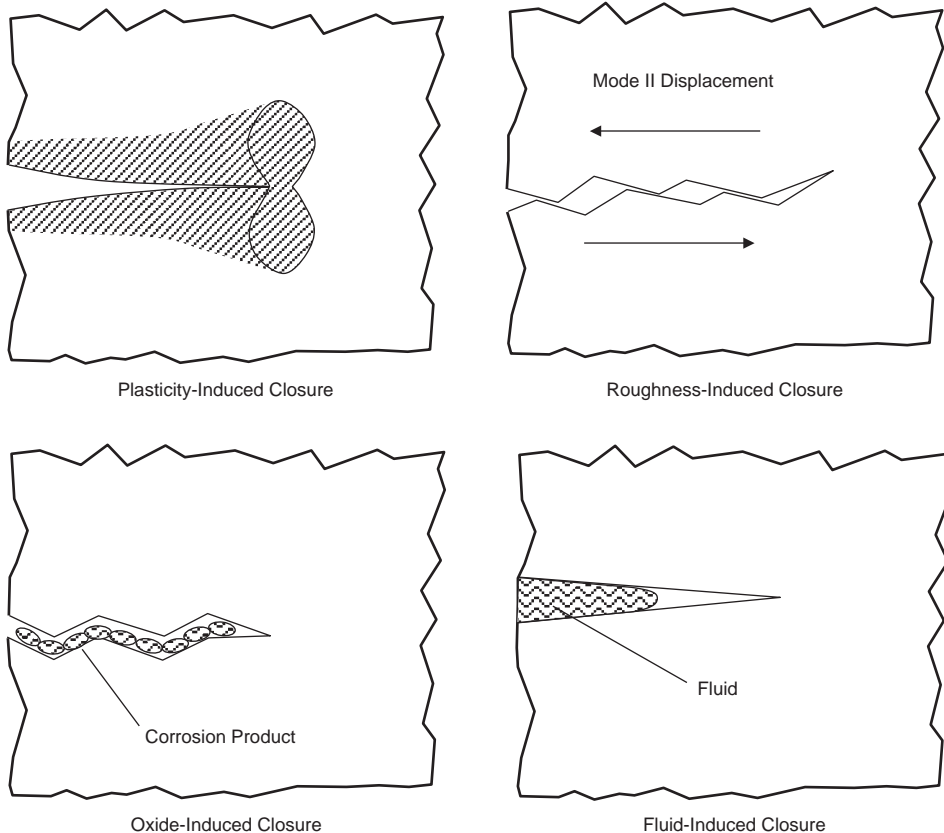


Fig. 14.20 Fatigue crack closure mechanisms in metals. Source: Ref 7

Notched fatigue data are also reported using a notch sensitivity factor, q :

$$q = \frac{K_f - 1}{K_t - 1} \quad (\text{Eq 14.24})$$

This relationship compares the theoretical stress-concentration factor, K_t , to the fatigue notch factor, K_f . In this relationship, a material that experiences no reduction in fatigue due to a notch will have a notch sensitivity factor of $q = 0$, while one that experiences a reduction in fatigue up to the full theoretical value will have a notch sensitivity factor of $q = 1$. The value of q is dependent on the material and the radius of the notch root, as illustrated by the plots shown in Fig. 14.22 for steels. The notch sensitivity factor, q , significantly decreases with smaller notch radii. Although this seems counterintuitive, it occurs because K_f increases more slowly than K_t with decreasing notch radius. For notches with large radii, K_f is almost equal to K_t . For materials with small notches, K_f is less than K_t . In addition, lower-strength metals are less affected than high-strength metals by geometric discontinuities that reduce the fatigue resistance, because high-strength metals have a limited capacity for deformation and crack tip blunting.

14.9 Manufacturing Stress Concentrations

Because almost all fatigue failures start on a surface, the surface finish and residual-stress state near the surface can have a profound effect

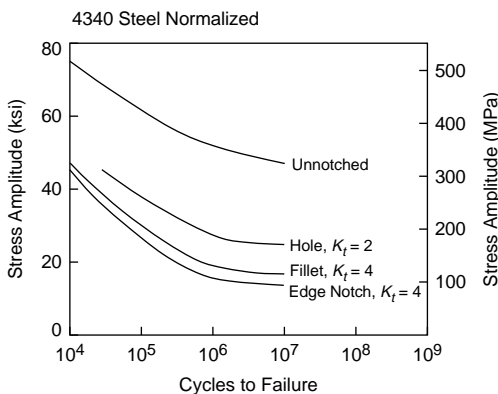


Fig. 14.21 Effect of geometrical stress concentrations on fatigue life. Source: Ref 8

on the fatigue strength. Since the early days of fatigue investigations, it was recognized that the fatigue life of a component is very dependent on the surface finish produced by machining or grinding operations. As shown in Fig. 14.23, highly polished steel specimens perform much better in fatigue than even carefully machined surfaces. Further degradation in fatigue strength occurs for hot rolled and forged surfaces. Finally, when corrosion is introduced, the fatigue life can be seriously degraded.

Parts that are formed at room temperature will contain residual stresses. For example, the surface of a part that was formed in tension will contain residual compressive stresses, and a surface that was in compression during forming will contain residual tensile stresses. Since fatigue always occurs under tensile loading, the surface with the residual tensile stresses will be the most prone to fatigue cracking. Similar to forming, some quenching operations during heat treatment can result in a tensile residual-stress pattern on the surface that will adversely affect fatigue strength.

The fatigue data shown in Table 14.1 for 4340 steel forgings tested in fully reversed bending illustrate two important points. First, vacuum melting, which removes inclusions, improves both the longitudinal and transverse endurance limits. Second, since forging tends to elongate inclusions in the longitudinal or working direction, the fatigue endurance limit is higher in the longitudinal direction. The lower transverse endurance limit in steels containing inclusions is attributed to stress concentrations at the inclusions, which can be quite high when an elongated stringer is oriented transverse to the tensile stress. For the case of the vacuum-melted steel, the transverse limit is still somewhat lower than

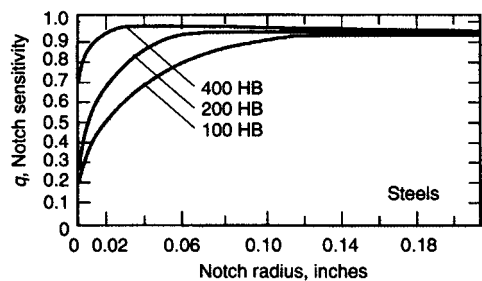


Fig. 14.22 Notch sensitivity versus notch radius for steels. Source: Ref 9

for the longitudinal direction, indicating the extreme sensitivity of transverse fatigue properties to microstructure.

Due to their extreme strength and hardness, high-strength steels are often finished by grinding to provide precise dimensions, remove any nicks or scratches, and provide smooth surfaces. However, great care must be taken when grinding these ultrahigh-strength steels. Improper or abusive grinding can result in grinding burns, in which the surface is heated above the austenitizing temperature and the austenite formed converts to untempered martensite on cooling (Fig. 14.24). This untempered martensitic surface layer is brittle and susceptible to forming a network of fine cracks that can reduce the fatigue strength by as much as 30%. Even if the grinding temperature is not high enough to produce austenite, it may cause the original tempered martensite microstructure on the surface to become overtempered, thereby reducing the strength and hardness.

14.10 Environmental Effects

Corrosion Fatigue. The simultaneous action of fatigue and corrosive attack is known as corrosion fatigue. In the absence of fatigue loading, corrosive attack can often cause pitting of a metal surface. These pits can then act as stress concentrations that will initiate fatigue cracking. When corrosion and fatigue occur simultaneously, the chemical attack greatly accelerates fatigue crack growth. Materials such as steels, which show a definite endurance limit when tested in air, do not exhibit a definite endurance limit when tested in a corrosive environment (Fig. 14.25). Frequently, fatigue will corrupt the protective films that would normally slow the corrosive attack, allowing continued and accelerated attack. Since corrosion is time dependent, slow cycling rates will result in greater life reductions than accelerated fatigue cycling. Another possible effect of a corrosive environment on fatigue life is the

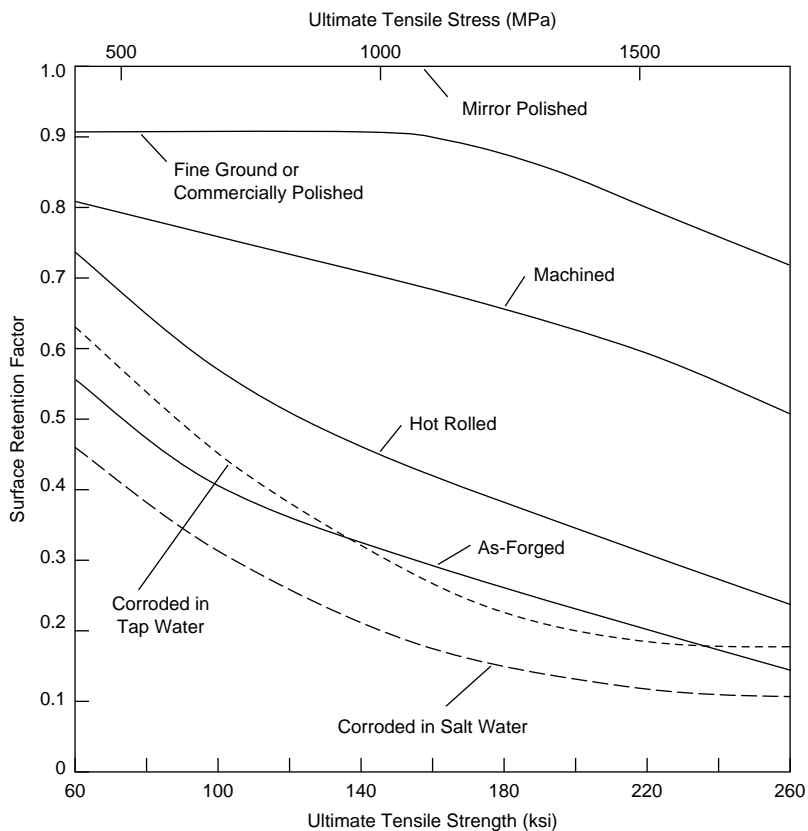


Fig. 14.23 Effect of surface finish on fatigue of steels. Source: Ref 10

Table 14.1 Effect of inclusions in 4340 forged steel

Property	Electric furnace melted	Vacuum melted
Longitudinal fatigue limit MPa (ksi)	800 (116)	960 (139)
Transverse fatigue limit MPa (ksi)	545 (79)	830 (120)
Ratio transverse/longitudinal	0.68	0.86
Hardness (HRC)	27	29

Source: Ref 11

absence of the stable stage II crack growth that occurs according to the Paris law. A reduction in fatigue life of 50% or more is not unusual.

There are a number of methods used to combat corrosion fatigue. First, the choice of a material for an aggressive environment should probably be based on its corrosion resistance rather than its fatigue properties. For example, stainless steel, bronze, or beryllium-copper would probably yield better service than heat treated steels. Corrosion-resistant coatings that isolate the surface from the environment are successful as long as the coating does not rupture during cycling. Zinc and cadmium coatings on steel and aluminum alclad coatings on aluminum generally produce better fatigue lives in aggressive environments, even though the coatings may reduce fatigue lives somewhat when tests are conducted in air. The introduction of surface compressive residual-stress patterns by shot peening or nitriding can be very useful.

Low-Temperature Fatigue. Fatigue life normally increases with decreasing temperatures. Although steels become more notch sensitive at low temperatures, there is no experimental evidence indicating that any sudden change in fatigue properties occurs at temperatures below the ductile-to-brittle transition temperature.

High-Temperature Fatigue. In general, the fatigue strength of metals decreases with increasing temperatures. An exception is mild steel, which exhibits a maximum in fatigue strength between 205 and 300 °C (400 and 575 °F) due to strain aging. As the temperature exceeds approximately half the melting point, T_m , creep can become the dominant cause of failure. Ferrous alloys, which usually exhibit an endurance limit at room temperature, will no longer have an endurance limit when the temperature exceeds approximately 425 °C (800 °F). In general, the higher the creep strength of an alloy, the higher will be its high-temperature fatigue strength. However, there are

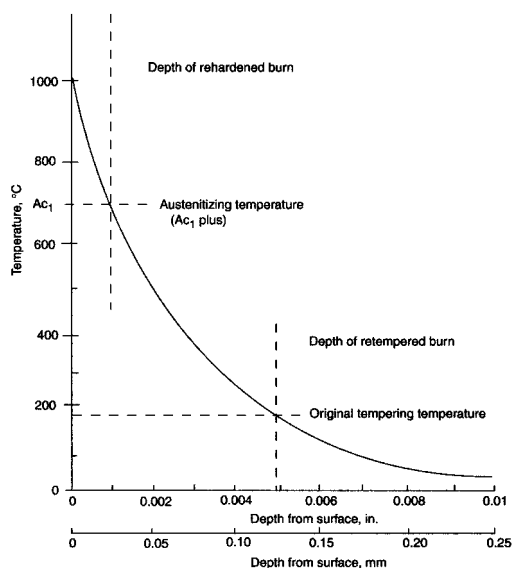
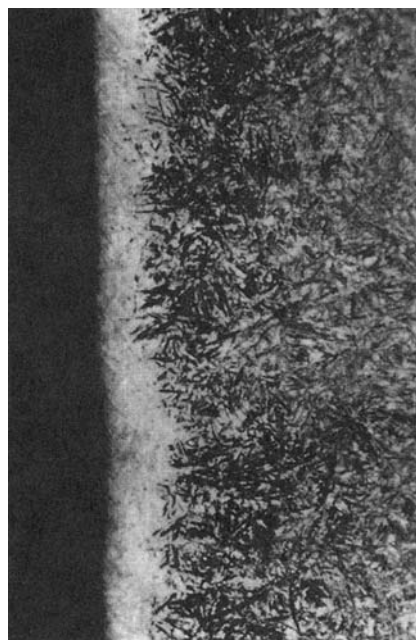


Fig. 14.24 Effects of grinding burns (untempered martensite) on high-strength steel. Source: Ref 12

conflicting requirements, with fine grain sizes being beneficial to fatigue properties, while coarse grain sizes are preferred in certain creep regimes. In addition, the beneficial effects of fatigue improvement processes such as shot peening, which are effective at room temperature, may be annealed out at elevated temperatures.

Thermal Fatigue. Thermal stresses result when dimensional changes in response to temperature changes are restricted by some type of constraint imposed on the component. For the case of a simple bar constrained rigidly at both ends, the thermal stress, σ , developed by a temperature change, ΔT , is:

$$\sigma = \alpha E \Delta T \quad (\text{Eq 14.25})$$

where α is the linear coefficient of thermal expansion, and E is the modulus of elasticity.

If failure occurs during one cycle of thermal stress because of a rapid temperature change, the phenomenon is known as thermal shock, while failures occurring after multiple thermal stress cycles caused by a cyclic temperature change are referred to as thermal fatigue. An example of thermal fatigue occurs in ceramic thermal barrier coatings that are applied to nickel-base superalloys used in jet engines. The large differences in the coefficients of thermal expansion of the ceramic coating and the underlying nickel blade result in cracking and spalling of the coating. Another example of thermal fatigue occurs in electronics. Heat generated during operation of electronic devices can cause fatigue of the soldered joints.

The tendency for thermal fatigue has been related to the parameter:

$$\sigma_f k / E \alpha \quad (\text{Eq 14.26})$$

where σ_f is the mean fatigue strength, and k is the thermal conductivity. A high value of this parameter indicates good resistance to thermal fatigue.

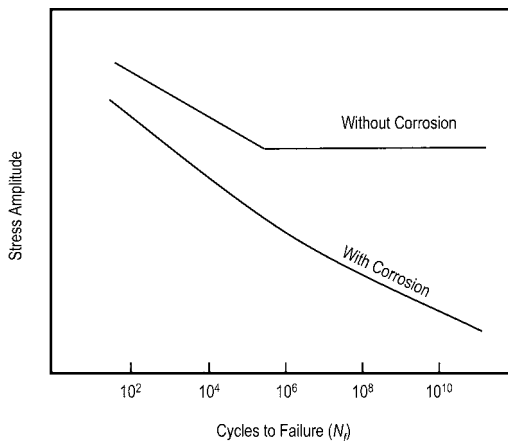


Fig. 14.25 Effect of corrosion on fatigue performance

14.11 Fatigue Life Improvement

One of the most effective methods of improving fatigue life is to induce residual compressive stresses on the surface of the part. This is often accomplished by shot peening or by surface rolling with contoured rollers. Shot peening involves propelling fine steel or cast iron shot into the surface at high velocities. The severity of the stress produced by shot peening is monitored by measuring the residual deformation of shot-peened specimens called Almen strips. In addition to inducing compressive stress on the surface, the surface layers are also strengthened by the cold working that occurs during shot peening. Important variables in shot peening include the hardness of the shot, the size, the shape, and the velocity. Shot peening must be carefully controlled so as not to introduce surface damage to the part. Shot peening

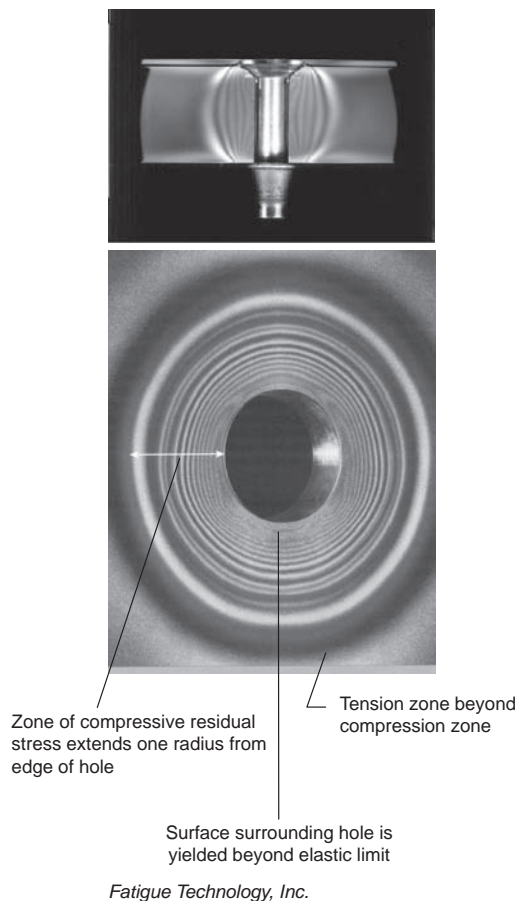


Fig. 14.26 Residual-stress state around cold-worked hole

imparts greater fatigue life during high-cycle fatigue than it does for higher-stress low-cycle fatigue. In low-cycle fatigue, large stresses in the plastic range cause “fading” of the residual-stress pattern.

Steel parts subjected to wear conditions are often carburized or nitrided to harden the surface for greater wear resistance. Since both of these processes also introduce residual compressive stresses on the surface, there is an improvement in fatigue life. The greatest improvement occurs where a high stress gradient occurs, as in bending or torsion, with less improvement in axial loading. Nitriding is extremely effective in improving the fatigue strength of notched specimens. Other surface-hardening methods, such as flame or induction hardening, produce similar effects. Case hardening is more effective for components that have a stress gradient, as in bending, or where there is a notch. For axially loaded components, fatigue cracks can form under the case in the softer, weaker core at the boundary between the surface and bulk.

Many large structures are assembled with mechanical fasteners. In the aerospace industry, fatigue life improvement of aluminum structures is often accomplished with cold working of fastener holes and/or installing interference fit fasteners. Since fatigue cracks often initiate at

fastener holes in metallic structures, methods such as cold working fastener holes and interference fit fasteners have been developed to improve fatigue life. Both cold working and interference fit fasteners set up residual compressive stress fields in the metal immediately adjacent to the hole (Fig. 14.26). The applied tension stress during fatigue loading must then overcome the residual compressive stress field before the hole becomes loaded in tension. The fatigue improvement due to cold working in 2024-T851 aluminum is shown in Fig. 14.27.

Cold working of holes is usually conducted using either the split-sleeve or split-mandrel method. Both methods involve pulling a mandrel through the hole that expands the hole diameter, creating plastic deformation of material around the hole and a resulting residual compressive stress field. The residual-stress field, depending on the material and the amount of expansion, will extend approximately one radius from the edge of the hole. In the split-sleeve process (Fig. 14.28), a stainless steel split sleeve is placed over a tapered mandrel and inserted into the hole. The hole is cold worked when the largest part of the mandrel is drawn back through the sleeve. After cold working, the sleeve is removed and discarded. In the split-mandrel process, a collapsible mandrel is placed in the

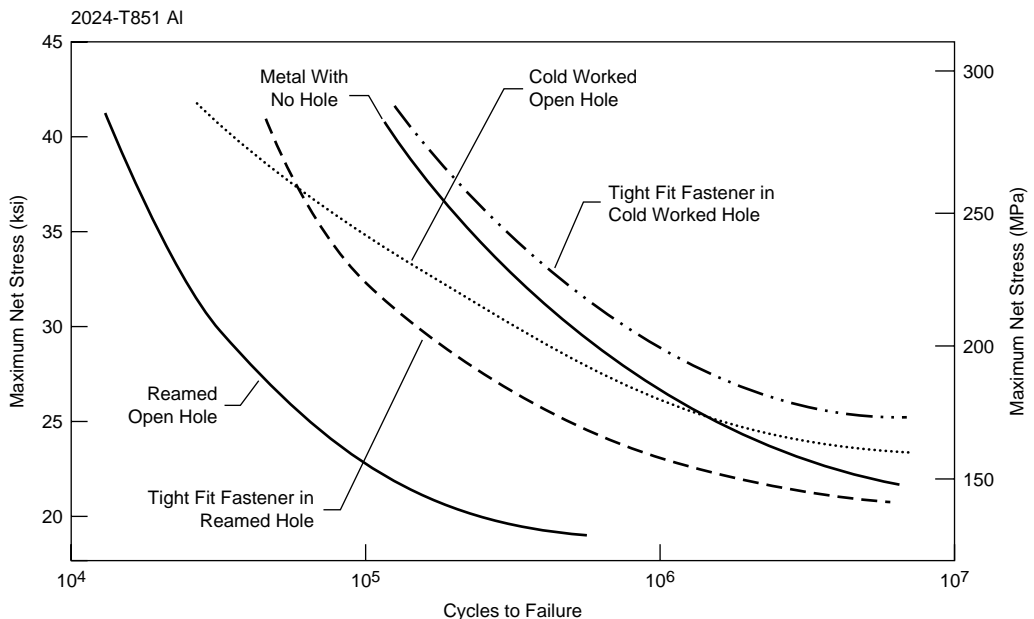


Fig. 14.27 Fatigue life improvement with cold working. Source: Ref 13

262 / Elements of Metallurgy and Engineering Alloys

hole, and as the mandrel is withdrawn, it expands to cold work the hole.

Interference fit fasteners can also be used in metallic structures to improve fatigue life. When an interference fit fastener is installed in metal, it also plastically deforms a small zone around the hole, setting up a compressive stress field, which again is beneficial when fatigue loading is primarily tensile. The amount of interference can vary, depending on structural requirements, but it is usually in the range of 0.07 to 0.10 mm (0.003 to 0.004 in.). In some highly loaded holes, both cold working and interference fit fasteners are used. While cold working and the use of interference fit fasteners are proven methods of improving fatigue resistance, both increase assembly costs and should only be specified when they are really needed.

Castings can be hot isostatic pressed (HIP) to help reduce internal porosity. The HIP of aluminum castings is usually conducted using

argon pressure at 105 MPa (15 ksi) and temperatures in the range of 480 to 525 °C (900 to 980 °F). The use of HIP usually results in improved mechanical properties, especially fatigue strength, but, of course, it adds to the cost and cycle time. The improvement in fatigue life for the aluminum casting alloy A201.0-T7 as a result of HIP is shown in Fig. 14.29.

14.12 Fatigue Design Methodologies

Since the 1800s, a number of design philosophies or methodologies have evolved to deal with design against fatigue failures.

Infinite-Life Design. This is the oldest of the design philosophies and is based on maintaining the stresses at some fraction below the fatigue strength of the metal. The initial material is assumed to be free of flaws. This methodology is based on the classic *S-N* curve. It is most

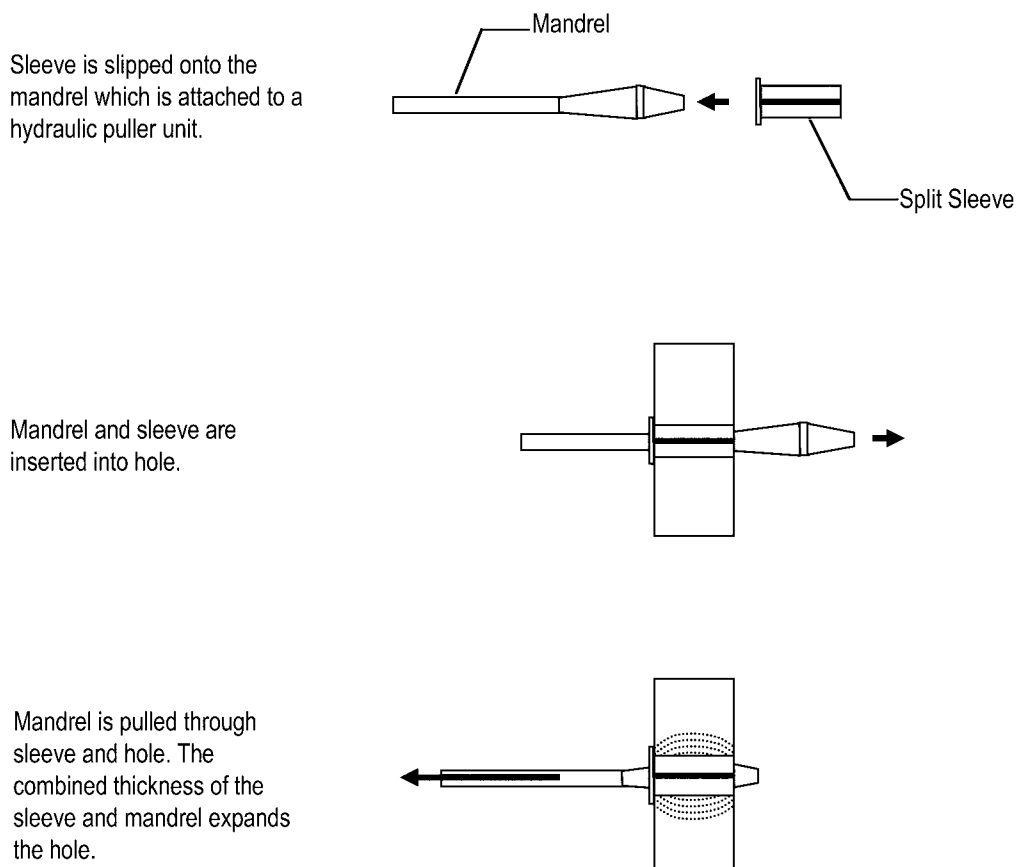


Fig. 14.28 Split-sleeve cold working process. Reprinted with permission from SAE Paper # 982145 © 1998 SAE International. Source: Ref 14

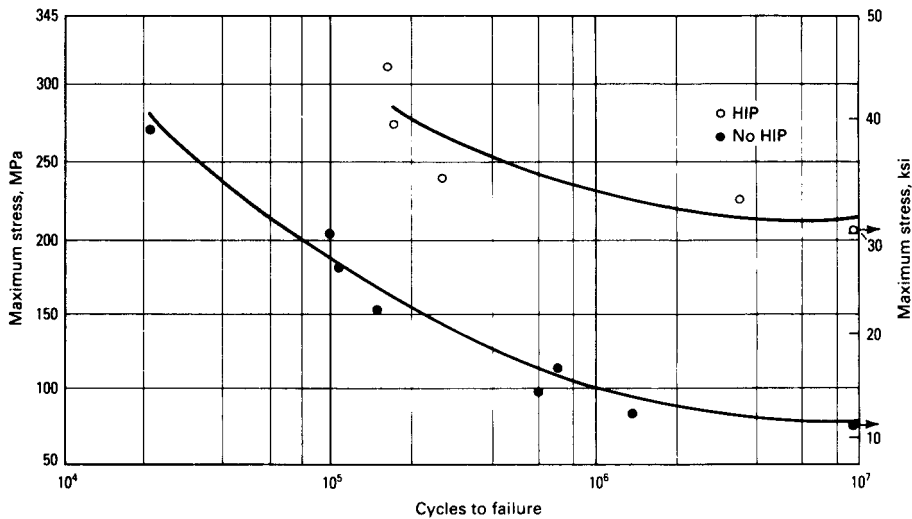


Fig. 14.29 Effect of hot isostatic pressing (HIP) on fatigue life of A201.0-T7 aluminum casting. Source: Ref 15

applicable when the component is only stressed in the elastic range and displays a distinct endurance limit, such as for steels. Although it has largely been superseded by later methodologies, it is simple to use and can be useful where periodic inspection is either impractical or not warranted. However, since it is a conservative methodology, it usually results in a heavier design than some of the later methodologies.

Safe-life design is based on the assumption that the part is initially flaw-free and has a finite life in which to develop a critical crack size. Like the infinite-life methodology, safe-life assumes an initial flaw-free component. This methodology was developed to account for parts that were subjected to higher loads that produced plastic strains. Under these conditions, the description of local events in terms of strain made more sense and resulted in the development of assessment techniques that used strain as a determining quantity, that is, log strain (ϵ) versus log number of cycles (N). The failure criterion is usually the detection of a small crack or some equivalent measure related to a substantial change in load-deflection response, although failure may also be defined as fracture.

Fail-Safe Design. The fail-safe design philosophy assumes that fatigue cracks will be detected and repaired before they lead to failure. This methodology was developed in the aircraft industry where large safety margins were weight-prohibitive. Fail-safe designs

incorporate multiple load paths and crack stoppers in the structure. In other words, if a primary load path fails, the load will be picked up by an alternate load path to prevent the structure from failing. A major part of this methodology is rigid certification criteria along with the capability to detect and inspect cracks.

Damage-tolerant design is the latest design methodology and is an extension of fail-safe design. The refinement of the damage-tolerant methodology is the assumption that structures do contain cracks and that fracture mechanics approaches can be used to determine crack growth rates. If the crack growth rate can be calculated, it is then possible to inspect the structure at various intervals and either repair or retire it prior to the crack reaching critical dimensions.

Although much progress has been made in the design against fatigue failures, they still occur with disturbing frequency. For any design, it is imperative that part or component testing be conducted prior to placing the part in service. In addition, it is important that the test conditions are representative of the actual environment that the component will experience in service.

REFERENCES

1. Fatigue Failures, *Failure Analysis and Prevention*, Vol 11, *ASM Handbook*, ASM International, 2002

264 / Elements of Metallurgy and Engineering Alloys

2. S. Kalpakjian, *Manufacturing Engineering and Technology*, 3rd ed. Addison-Wesley Publishing Co., 1995
3. *Properties and Selection of Metals*, Vol 1, *Metals Handbook*, 8th ed., American Society for Metals, 1961
4. R.A. Higgins, *Engineering Metallurgy—Applied Physical Metallurgy*, 6th ed., Arnold, 1993
5. M.A. Meyers and K.K. Chawla, *Mechanical Metallurgy—Principles and Applications*, Prentice-Hall Inc., 1984
6. C.M. Laird, STP 415, American Society for Testing and Materials, 1966, p 130
7. T.L. Anderson, *Fracture Mechanics: Fundamentals and Applications*, 3rd ed., Taylor & Francis, 2005
8. J. Collins and S. Daniewicz, Failure Considerations, *Mechanical Engineers Handbook*, John Wiley & Sons, Inc., 1998
9. M.R. Mitchell, Fundamentals of Modern Fatigue Analysis for Design, *Fatigue and Fracture*, Vol 19, *ASM Handbook*, ASM International, 1996
10. R.C. Juvinall, *Stress, Strain, and Strength*, McGraw-Hill Book Co., 1967
11. G.E. Dieter, *Mechanical Metallurgy*, 3rd ed., McGraw-Hill Book Co., 1986, p. 375–431
12. G.E. Toten, et al., Factors Relating to Heat Treating Operations, *Failure Analysis and Prevention*, Vol 11, *ASM Handbook*, ASM International, 2002
13. F.C. Campbell, *Manufacturing Technology for Aerospace Structural Materials*, Elsevier Scientific, 2006
14. A. Leon, “Developments in Advanced Coldworking,” SAE 982145, Society of Automotive Engineers, 1998
15. J.R. Davis, *ASM Specialty Handbook: Aluminum and Aluminum Alloys*, ASM International, 1993

SELECTED REFERENCES

- M.F. Ashby and D.R.H. Jones, *Engineering Materials 1 — An Introduction to Their Properties and Applications*, 2nd ed., Butterworth Heinemann, 1996
- T.H. Courtney, *Mechanical Behavior of Materials*, 2nd ed., McGraw-Hill Book Co., 2000, p 566–629
- H.W. Hayden, W.G. Moffatt, and J. Wulf, *The Structure and Properties of Materials*, Vol III, John Wiley, 1965
- M.P. Kaplan and T.A. Wolff, Fatigue-Life Assessment, *Failure Analysis and Prevention*, Vol 11, *ASM Handbook*, ASM International, 2002
- E. Krempl, Design for Fatigue Resistance, *Materials Selection and Design*, Vol 20, *ASM Handbook*, ASM International, 1997
- R.A. Lund and S. Sheybany, Fatigue Fracture Appearances, *Failure Analysis and Prevention*, Vol 11, *ASM Handbook*, ASM International, 2002



ASM International is the society for materials engineers and scientists, a worldwide network dedicated to advancing industry, technology, and applications of metals and materials.

ASM International, Materials Park, Ohio, USA
www.asminternational.org

This publication is copyright © ASM International®. All rights reserved.

Publication title	Product code
Elements of Metallurgy and Engineering Alloys	05224G

To order products from ASM International:

Online Visit www.asminternational.org/bookstore

Telephone 1-800-336-5152 (US) or 1-440-338-5151 (Outside US)

Fax 1-440-338-4634

Mail Customer Service, ASM International
9639 Kinsman Rd, Materials Park, Ohio 44073-0002, USA

Email CustomerService@asminternational.org

In Europe American Technical Publishers Ltd.
27-29 Knowl Piece, Wilbury Way, Hitchin Hertfordshire SG4 0SX,
United Kingdom
Telephone: 01462 437933 (account holders), 01462 431525 (credit card)
www.ameritech.co.uk

In Japan Neutrino Inc.
Takahashi Bldg., 44-3 Fuda 1-chome, Chofu-Shi, Tokyo 182 Japan
Telephone: 81 (0) 424 84 5550

Terms of Use. This publication is being made available in PDF format as a benefit to members and customers of ASM International. You may download and print a copy of this publication for your personal use only. Other use and distribution is prohibited without the express written permission of ASM International.

No warranties, express or implied, including, without limitation, warranties of merchantability or fitness for a particular purpose, are given in connection with this publication. Although this information is believed to be accurate by ASM, ASM cannot guarantee that favorable results will be obtained from the use of this publication alone. This publication is intended for use by persons having technical skill, at their sole discretion and risk. Since the conditions of product or material use are outside of ASM's control, ASM assumes no liability or obligation in connection with any use of this information. As with any material, evaluation of the material under end-use conditions prior to specification is essential. Therefore, specific testing under actual conditions is recommended.

Nothing contained in this publication shall be construed as a grant of any right of manufacture, sale, use, or reproduction, in connection with any method, process, apparatus, product, composition, or system, whether or not covered by letters patent, copyright, or trademark, and nothing contained in this publication shall be construed as a defense against any alleged infringement of letters patent, copyright, or trademark, or as a defense against liability for such infringement.